

PERFORMANCE EVALUATION OF HYBRID RF/FSO SYSTEMS USING NAKAGAMI-M AND GAMMA-RICIAN MODELS FOR ONE-HOP AND MULTI-HOP SCENARIOS

Dorđe Šarčević¹ – Nenad Stanojević^{2*} – Stefan Panić³ – Petar Spalević² – Nikola Gligorijević⁴ – Čedomir Vasić⁵

¹ Academy of Professional Studies Šabac, Dobropoljska 5, 15000 Šabac, Serbia

² Faculty of Technical Sciences, University of Priština, Knjaza Miloša 7, 38220 Kosovska Mitrovica, Serbia

³ Faculty of Sciences and Mathematics, University of Priština, Lole Ribara 29, 38220 Kosovska Mitrovica, Serbia

⁴ Faculty of Information Technology, Alfa BK University, Bulevar Maršala Tolbuhina 8, 11000 Beograd, Serbia

⁵ Information-Technology-FBL, MB University, Teodora Dražera 27, 11000 Beograd, Serbia

ARTICLE INFO

Article history:

Received: 27. 9. 2025.

Received in revised form: 8. 11. 2025.

Accepted: 8. 11. 2025.

Keywords:

Gamma-Rician model

Hybrid RF/FSO systems

Multi-Hop transmission

Nakagami-m fading

DOI: 10.30765/er.3060

Abstract:

In this study, a comprehensive model for evaluating the performance of hybrid RF/FSO (Radio Frequency/Free Space Optics) systems is introduced. The recently presented Gamma-Rician model was employed for the statistical characterisation of FSO turbulence, while the Nakagami-m fading model was utilised for RF propagation modelling. We provide closed-form expressions for the Cumulative Distribution Function (CDF) of observed Signal-to-Noise Ratio (SNR) at reception, along with closed-form expressions for the Average Bit Error Rate (ABER) using the Coherent Binary Phase Shift Keying (CBPSK) modulation scheme. Two transmission methods in relay hybrid RF/FSO systems have been analysed: One-Hop and Multi-Hop transmissions. By capitalising on these expressions, we have evaluated the ABER performance of these systems as a function of various parameters, highlighting the robustness of hybrid configurations under differing operational conditions.

1 Introduction

Free space optics (FSO) and Radio Frequency (RF) hybrid communication systems have garnered significant attention due to their potential to synergise the high bandwidth and low latency of FSO with the robustness and extensive coverage of RF technologies. Foundational works, such as Chowdhury et al. (2020) [1], provide comprehensive surveys on optical wireless hybrid networks, emphasising the complementary characteristics of RF and optical wireless communication (OWC) technologies. These studies underscore the potential of hybrid systems to support emerging 5G networks and beyond by leveraging various combinations of RF and optical technologies, including Visible Light Communication (VLC), Light Fidelity (LiFi), Optical Camera Communication (OCC), and FSO. Performance analysis and channel modelling form a crucial aspect of understanding hybrid systems. Khalighi et al. (2014) [2] delve into the challenges posed by atmospheric turbulence and alignment in FSO systems, advocating for hybrid approaches to mitigate these issues. Technological advancements in Optical Wireless Communications (OWC), particularly in indoor scenarios, have been reviewed by Elgala et al. (2011) [3], highlighting the integration of VLC and LiFi with RF systems. Sevincer et al. (2013) [4] explore the potential of combining VLC and FSO technologies, demonstrating significant improvements in data transmission and security. Furthermore, Xu et al. (2008) [5] provide insights into ultraviolet (UV) communications, which, although distinct, offer relevant channel modelling and environmental impact considerations applicable to FSO. Recent studies continue to showcase the efficacy of

* Corresponding author

E-mail address: nenads25@gmail.com

RF/FSO hybrid systems in dynamically adjusting to real-time conditions, thereby ensuring robust and uninterrupted communication.

FSO and RF hybrid communication systems synergise the advantages of both technologies to address their respective limitations, offering a robust solution for modern communication needs [6], [7]. FSO systems utilise light beams in the infrared spectrum to transmit data, providing high bandwidth, low latency, and immunity to electromagnetic interference. These attributes make FSO systems ideal for deployment in urban environments. However, FSO systems are highly sensitive to atmospheric conditions such as fog, dust, and turbulence, which can severely degrade or even interrupt the signal. Furthermore, precise alignment of the optical devices is crucial, posing significant challenges in installations on tall buildings where wind-induced sway can cause signal jitter. In contrast, RF communication systems, while generally having lower data rates and bandwidth than FSO, are more resilient in adverse weather conditions, maintaining communication through clouds and fog. This robustness ensures continuous data transmission when FSO signals are compromised. By combining these two technologies into a hybrid RF/FSO system, it is possible to leverage the high-speed capabilities of FSO during favourable conditions and the reliability of RF during unfavourable conditions, thereby enhancing the overall performance and reliability of the communication system. The integration of RF and FSO technologies is most commonly realised through relay technology, where different segments of the transmission path use FSO or RF depending on the prevailing conditions. Relay stations play a crucial role in these systems by continuously monitoring transmission conditions and dynamically switching between FSO and RF links to ensure optimal performance. When atmospheric conditions are optimal, the FSO link is utilized for its superior data rates and low latency. Conversely, under adverse conditions, the RF link takes over to maintain reliable data transmission. There are two primary configurations for these hybrid systems: One-Hop and Multi-Hop. In a One-Hop system, data is transmitted directly from the transmitter to the receiver. This configuration balances high performance and reliability, making it suitable for scenarios that require consistent high-speed transmission regardless of weather conditions. Multi-Hop systems, on the other hand, represent a more advanced level of wireless communication, utilising multiple relay stations. Each relay station receives, analyses, amplifies, and forwards the signal to the next station, thereby extending the propagation distance and overcoming the limitations of direct transmission. Multi-Hop networks can be implemented using parallel, series, or combined configurations, each offering distinct advantages in terms of robustness and performance [8].

In [9] Rakia et al. (2015) introduce a practical FSO/RF hybrid system with adaptive combining. This study presents a novel transmission scheme where the FSO link is utilised as long as its signal-to-noise ratio (SNR) is above a certain threshold. When the FSO link's quality degrades, the RF link is activated, and the signals from both links are combined using a dual-branch maximal-ratio combiner. The authors derive a novel analytical expression for the cumulative distribution function (CDF) of the received SNR, which is used to study the system's outage performance. The results demonstrate significant improvements in outage performance compared to FSO-only and RF-only systems, particularly in clear and adverse weather conditions. In [10], Mohammed J. Sabre et al. (2019) investigate the secrecy performance of a mixed RF-FSO cooperative relaying system using α - μ and Exponentiated Weibull fading models. The authors analyse the secrecy outage probability and secure transmission probability under different fading conditions, providing insights into the security advantages of hybrid RF-FSO systems. This research emphasises the importance of considering various fading models to accurately assess the performance and security of hybrid communication systems. The findings reveal that hybrid systems can offer enhanced secrecy performance, making them suitable for secure communication applications. In addition, the work by Bassam Helal et al. (2019) [11] focuses on the practical implementation aspects of hybrid RF/FSO systems. The study explores various relay-assisted hybrid architectures and their performance under different environmental conditions. By employing different modulation schemes and diversity combining techniques, the authors demonstrate how hybrid systems can dynamically adapt to changing atmospheric conditions to maintain reliable communication links. This research provides a comprehensive framework for designing and optimising hybrid RF/FSO systems to achieve high data rates and reliability.

In order to evaluate the characteristics of RF/FSO systems, it is necessary to perform statistical modelling of relay hybrid RF/FSO systems. In the paper [12], a new relay hybrid RF/FSO model is presented, based on the Nakagami-m distribution for RF fading and the Gamma-Gamma distribution for the FSO turbulence channel. This paper presents the results of calculating Average Bit-Error Rate (ABER) and Outage Probability (OP) for both types of transmission systems, One-Hop and Multi-Hop. The analysis of the results shows that

One-Hop RF/FSO systems exhibit significantly better characteristics than the FSO transmission system. It was also found that the implementation of Multi-Hop systems further enhances the characteristics of the hybrid RF/FSO system. In the paper [13], a hybrid RF/FSO system is presented, in which the primary FSO link is modelled using the Gamma-Gamma statistical model, while the backup RF fading is modelled using the Rayleigh distribution. The analysis of ABER and OP, and the comparison with the results of the FSO communication system, showed that the presented system provides better results in all weather conditions. In a similar manner, this paper presents a new relay hybrid RF/FSO statistical model for analysing the performance of transmission systems. The Nakagami- m statistical model is used for modelling RF fading, while the Gamma-Rice statistical model is used for modelling the FSO communication channel. For the purpose of result analysis, ABER was determined using the Coherent Binary Phase Shift Keying (CBPSK) modulation scheme. The paper is organised into three sections. In the first section, the procedure for obtaining the new CDF is presented. In the second section, expressions for ABER for One-Hop and Multi-Hop relay hybrid systems are presented, as well as the basic expression for the transmission of the FSO communication channel. In the third section, the results for ABER of FSO and RF/FSO communication systems are presented and discussed. The results of ABER are analysed for different weather conditions and for different values of system parameters.

2 System and channel model

2.1 Modelling of RF fading

For modelling RF fading, the Probability density function (PDF) of the Nakagami- m distribution is used, which can be represented by the expression [14]:

$$f_{Y_{RF}}(Y_{RF}) = \left(\frac{m^m Y_{RF}^{m-1}}{\Gamma(m) \mu_{RF}^m} \right) e^{-\frac{mY_{RF}}{\mu_{RF}}} \quad (1)$$

where m is the fading statistics factor and its value is always $m \geq 0.5$, μ_{RF} denotes the average SNR, and $\Gamma(\cdot)$ represents the Gamma function.

Expression (1) can also be represented and used using the Meijer G function [16]:

$$f_{Y_{RF}}(Y_{RF}) = \left(\frac{m}{\mu_{RF}} \right)^m \left(\frac{Y_{RF}^{m-1}}{\Gamma(m)} \right) G_{0.1}^{1.0} \left(0 \left| \frac{mY_{RF}}{\mu_{RF}} \right. \right) \quad (2)$$

The CDF expression is obtained by solving the integral [15]:

$$F_{Y_{RF}}(Y_{RF}) = \int_0^{Y_{RF}} f_{Y_{RF}}(Y_{RF}) dY_{RF} \quad (3)$$

By substituting expression (2) into expression (3), applying rule (07.34.21.0084.01) from [16], the following equation is obtained:

$$F_{Y_{RF}}(Y_{RF}) = \left(\frac{1}{\Gamma(m)} \right) G_{1.2}^{1.1} \left(\frac{1}{m}, 0 \left| \frac{mY_{RF}}{\mu_{RF}} \right. \right) \quad (4)$$

The obtained result represents the CDF of the Nakagami- m distribution represented using the Meijer G function [16].

2.2 Modelling of FSO fading

For modeling the FSO link, the Gamma-Rice statistical model is used. The expression for the PDF under the influence of positioning error relative to SNR can be represented by the expression [17]:

$$f_{\gamma_{FSO}}(\gamma_{FSO}) = \sum_{p=0}^{\infty} \frac{\xi^2 K^p \exp(-K)}{2\gamma_{FSO} \Gamma(p+1) p! \Gamma(\alpha)} G_{1.3}^{3.0} \left(\begin{matrix} 1 + \xi^2 \\ \xi^2, \alpha, p + 1 \end{matrix} \middle| \frac{(K+1)\xi^2 \alpha}{(\xi^2+1)} \sqrt{\frac{\gamma_{FSO}}{\mu_{FSO}}} \right) \quad (5)$$

where K is the Rice factor, indicating the ratio of the dominant component to the components resulting from scattering, $\xi = w_{L,eq}/2\sigma_s$, w_L is the equivalent radius of the beam at the receiver, and σ_s denotes the standard deviation values of the displacement error (jitter) at the receiver. $w_{L,eq}$ is the equivalent diameter of the receiving aperture and can be represented by the expression:

$$w_{L,eq}^2 = w_L^2 \frac{\operatorname{erf}(v) \sqrt{\pi}}{2v} \exp(v^2) \quad (6)$$

where $v = \frac{\sqrt{\pi} a}{\sqrt{2} w_L}$, $A_0 = [\operatorname{erf}(v)]^2$, $\operatorname{erf}(\cdot)$ denotes the error function, α represents the number of large eddies in the scattering process, and can be represented by the expression:

$$\alpha = \frac{1}{\frac{0.49 \sigma_R^2}{e^{(1+1.1 \sigma_R^{12/5})^{5/6} - 1}}} \quad (7)$$

where $\sigma_R^2 = 1.23 C_n^2 k^{7/6} L^{11/6}$ is Rytov variance, C_n^2 is the refractive index commonly used to define turbulence strength, $k = 2\pi/\lambda$ denotes the wave number, and L denotes the propagation distance. The CDF can be obtained from the expression:

$$F_{\gamma_{FSO}}(\gamma_{FSO}) = \int_0^{\gamma_{FSO}} f_{\gamma_{FSO}}(\gamma_{FSO}) d\gamma_{FSO} \quad (8)$$

By substituting equation (5) into equation (8), we obtain the expression for the CDF:

$$F_{\gamma_{FSO}}(\gamma_{FSO}) = \sum_{p=0}^{\infty} \frac{2^{p+\alpha-2} \xi^2 K^p \exp(-K)}{\pi \Gamma(p+1) p! \Gamma(\alpha)} G_{2.6}^{5.1} \left(\begin{matrix} A \\ B, 0 \end{matrix} \middle| \frac{(K+1)^2 \xi^4 \alpha^2 \gamma_{FSO}}{16(\xi^2+1)^2 \mu_{FSO}} \right) \quad (9)$$

where $A = 1, \frac{2+\xi^2}{2}$ and $B = \frac{\xi^2}{2}, \frac{\alpha}{2}, \frac{\alpha+1}{2}, \frac{p+1}{2}, \frac{p+2}{2}$

3 Statistical characteristics of the RF/FSO system based on selective combination

By adopting a selective combination scheme that is implemented by comparing the SNR of the RF/FSO system with the maximum output SNR [18]:

$$\gamma = \max(\gamma_{RF}, \gamma_{FSO}) \quad (10)$$

γ_{RF} and γ_{FSO} are the SNR of the RF and FSO systems, respectively. The CDF as a function of SNR for the hybrid RF/FSO system can be represented by the equation:

$$F_{\gamma}(\gamma) = P_r(\max(\gamma_{RF}, \gamma_{FSO}) \leq \gamma) = P_r(\gamma_{RF} \leq \gamma, \gamma_{FSO} \leq \gamma) = F(\gamma_{RF})F(\gamma_{FSO}) \quad (11)$$

By substituting equations (4) and (9) into equation (11) and applying the rule for the product of two independent Meijer functions, we obtain the EGBMGF – Extended Generalized Bivariate Meijer-G Function, Eq. (07.34.16.0003.01) from [16]. This expression represents the CDF of the hybrid RF/FSO system:

$$F(\gamma) = \sum_{p=0}^{\infty} \frac{2^{p+\alpha-2} \xi^2 K^p \exp(-K)}{\pi \Gamma(p+1) p! \Gamma(\alpha)} G_{0,0}^{0,0} \begin{matrix} 1,1 \\ 1,2 \end{matrix} \begin{matrix} 5,1 \\ 2,6 \end{matrix} \left(\begin{matrix} 1 \\ m, 0 \end{matrix} \middle| \begin{matrix} A \\ B, 0 \end{matrix} \middle| \begin{matrix} m \\ \mu_{RF} \end{matrix} \middle| \begin{matrix} (K+1)^2 \xi^4 \alpha^2 \gamma_{FSO} \\ 16(\xi^2+1)^2 \mu_{FSO} \end{matrix} \right) \quad (12)$$

3.1 ABER for one-hop transmission systems

The expression for determining ABER is obtained by solving the integral [19], [20]:

$$P_{ABER}(\gamma) = \frac{\gamma^x}{2\Gamma(x)} \int_0^{\infty} e^{-\gamma\gamma} \gamma^{x-1} F_{\gamma}(\gamma) d\gamma \quad (13)$$

where $x=0.5$ and $y=1$ are parameters of the CBPSK modulation technique. By substituting equation (9) into equation (13) and applying the CBPSK modulation scheme, then solving the integral using rule (07.34.21.0088.01) from [16], the expression for ABER of the FSO transmission system is obtained:

$$P_{\gamma_{FSO}}(\gamma_{FSO}) = \sum_{p=0}^{\infty} \frac{2^{p+\alpha-3} \xi^2 K^p \exp(-K)}{\pi \Gamma(p+1) p! \Gamma(\alpha) \Gamma(x)} G_{3,6}^{5,2} \left(\begin{matrix} \frac{1}{2}, A \\ B, 0 \end{matrix} \middle| \begin{matrix} (K+1)^2 \xi^4 \alpha^2 \\ 16(\xi^2+1)^2 \mu_{FSO} \end{matrix} \right) \quad (14)$$

The standard One-Hop transmission system, which is based on transmission from the source to the receiving node, can be obtained by substituting equation (12) into equation (13), applying the CBPSK modulation scheme, and using rule (07.34.21.0081.01) from [16] to derive the expression for ABER:

$$P_{\gamma_{OH}}(\gamma_{OH}) = \sum_{p=0}^{\infty} \frac{2^{b+p-3} \xi^2 K^p \exp(-K)}{\pi \Gamma(m) \Gamma(p+1) p! \Gamma(\alpha) \Gamma(x)} G_{1,0}^{0,1} \begin{matrix} 1,1 \\ 1,2 \end{matrix} \begin{matrix} 5,1 \\ 2,6 \end{matrix} \left(\begin{matrix} 0 \\ -1 \end{matrix} \middle| \begin{matrix} 1 \\ m, 0 \end{matrix} \middle| \begin{matrix} A \\ B, 0 \end{matrix} \middle| \begin{matrix} m \\ \mu_{RF} \end{matrix} \middle| \begin{matrix} (K+1)^2 \xi^4 \alpha^2 \\ 16(\xi^2+1)^2 \mu_{FSO} \end{matrix} \right) \quad (15)$$

3.2 ABER for multi-hop transmission systems

The hybrid Multi-Hop RF/FSO system implemented using the Decode and Forward (DF) [21], [22] method, where the equivalent n-th SNR can be represented by the expression [18]:

$$\gamma_{en} = \min(\gamma_{e1}, \gamma_{e2}, \dots, \gamma_{eN}) \quad (16)$$

The CDF of the n-th path equivalent SNR can be represented by the expression:

$$F_{en} = 1 - [1 - F_{\gamma}]^M \quad (17)$$

Selecting the scheme with the best path also denotes choosing the signal with the highest instantaneous SNR ratio:

$$\gamma_e = \max(\gamma_{no}, \gamma'_e) \quad (18)$$

where $\gamma'_e = \max_{n=1, \dots, N} \gamma_{en}$

FSO and RF systems have equal SNR in all links, an expression for the CDF depending on γ'_e can be derived:

$$F_{\gamma'_e}(\gamma) = [F_{ei}(\gamma)]^N = [1 - [1 - F_{\gamma}]^M]^N \quad (19)$$

$$F_{\gamma'_e}(\gamma) = \left[1 - \left[1 - \sum_{p=0}^{\infty} \frac{2^{b+p-3} \xi^2 K^p \exp(-K)}{\pi \Gamma(m) \Gamma(p+1) p! \Gamma(\alpha) \Gamma(x)} G_{1,0}^{0,1} \begin{matrix} 1,1 \\ 1,2 \end{matrix} \begin{matrix} 5,1 \\ 2,6 \end{matrix} \left(\begin{matrix} 0 \\ -1 \end{matrix} \middle| \begin{matrix} 1 \\ m, 0 \end{matrix} \middle| \begin{matrix} A \\ B, 0 \end{matrix} \middle| \begin{matrix} m \\ \mu_{RF} \end{matrix} \middle| \begin{matrix} (K+1)^2 \xi^4 \alpha^2 \\ 16(\xi^2+1)^2 \mu_{FSO} \end{matrix} \right) \right]^M \right]^N \quad (20)$$

By combining equation (19) and equation (11), the expression for the CDF of the Hybrid RF/FSO Multi-Hop transmission system is obtained:

$$F_{\gamma}(\gamma) = F_{\gamma} \left[1 - [1 - F_{\gamma}]^M \right]^N \quad (21)$$

By substituting equation (21) into equation (13), the expression for ABER for Multi-Hop hybrid transmission systems is obtained:

$$F_{\gamma}(\gamma) = \sum_{p=0}^{\infty} \frac{2^{b+p-3} \xi^2 K^p \exp(-K)}{\pi \Gamma(m) \Gamma(p+1) p! \Gamma(\alpha) \Gamma(x)} \sum_t^n L_t G_{1,0}^{0,1} \begin{matrix} 1,1 & 5.1 \\ 1,2 & 2.6 \end{matrix} \left(\begin{matrix} 0 & 1 \\ - & m, 0 \end{matrix} \middle| \begin{matrix} A \\ B, 0 \end{matrix} \middle| \begin{matrix} m \\ \mu_{RF} \end{matrix} \middle| \frac{(K+1)^2 \xi^4 \alpha^2 z_t}{16(\xi^2+1)^2 \mu_{FSO}} \right) \left[1 - \right. \\ \left. \left[1 - \sum_{p=0}^{\infty} \frac{2^{b+p-3} \xi^2 K^p \exp(-K)}{\pi \Gamma(m) \Gamma(p+1) p! \Gamma(\alpha) \Gamma(x)} G_{1,0}^{0,1} \begin{matrix} 1,1 & 5.1 \\ 1,2 & 2.6 \end{matrix} \left(\begin{matrix} 0 & 1 \\ - & m, 0 \end{matrix} \middle| \begin{matrix} A \\ B, 0 \end{matrix} \middle| \begin{matrix} m \\ \mu_{RF} \end{matrix} \middle| \frac{(K+1)^2 \xi^4 \alpha^2}{16(\xi^2+1)^2 \mu_{FSO}} \right) \right]^M \right]^N \quad (22)$$

where L_t is the weighting coefficient obtained by approximating the integral $\int_0^{\infty} \gamma^x e^{y\gamma} F_{\gamma}(\gamma) d\gamma$ using Gauss-Laguerre quadrature [18]:

$$L_t = \frac{(t+\frac{1}{2})z_t}{\{n!(n+1)^2 [L_{n+1}^{-1/2} z_t]^2\}} \quad (23)$$

z_t is the t -th root of the generalized Laguerre polynomial L_{n+1} [23].

4 Results and discussion

The following parameters were used to obtain the results: propagation distance $L=1000$ m, wavelength $\lambda=1550$ nm, and refractive index, which is characteristic for weak, moderate, and strong turbulence, respectively $C_n^2 = 6 \times 10^{-15} m^{-2/3}$, $C_n^2 = 2 \times 10^{-1} m^{-2/3}$, $C_n^2 = 1.2 \times 10^{-1} m^{-2/3}$, standard deviation of the noise $\sigma_N=10^{-7}$, radius of the circular detector $a=0.05$ m, radius of the optical beam (dependent on distance) $w_L[m]=0.5$, standard deviation (jitter) at the receiver $\sigma_s=0.2$ m, fading statistics factor $m=2$. By substituting the corresponding parameters into equations (14) and (15), the graphs for the FSO system and One-Hop hybrid RF/FSO is obtained, considering the application of different values of the K factor depending on the electrical SNR under weak turbulence conditions. As anticipated from Figure 1, lower K -factor values and electrical SNR correlate with higher ABER levels, suggesting suboptimal system performance. Elevating the K factor decreases the ABER, thereby enhancing the FSO system's performance. Figure 2 shows that hybrid One-Hop RF/FSO systems outperform FSO systems, and their performance improves as SNR increases. The graph indicates that turbulence strength has little impact on RF/FSO system performance.

During periods of higher atmospheric turbulence, FSO system performance deteriorates, and signal transmission is taken over by the RF system, which is more resilient to turbulence. Figure 3 shows the relationship between ABER and the use of hybrid One-Hop models with Gamma-Rician distribution and Nakagami- m fading, and with Gamma-Gamma distribution and Nakagami- m fading, under different displacement-error influences. From Figure 3, it is evident that for lower SNR values, the pointing error has minimal impact on system performance. As SNR increases, system performance improves, but the effect of pointing error becomes more pronounced. Additionally, a comparative analysis was conducted between two different models under moderate turbulence conditions. Figures 4 and 5 show the presented One-Hop and Multi-Hop hybrid system under moderate turbulence for various values of the fading statistics parameter m . From Figure 4, it can be observed that lower values of the parameter m result in higher ABER values, indicating poorer system performance. Figure 5 presents the characteristics of the system using a parallel hybrid RF/FSO Multi-Hop system with $M=2$ hops and $N=3$ paths. This graph considers various values of the parameter m in relation to the electrical SNR. The graphs show that the hybrid RF/FSO Multi-Hop system exhibits significantly better results compared to the hybrid One-Hop RF/FSO system (figure 4). The model presented in this study demonstrates excellent performance improvements with increasing parameter m , as expected. Figures 6 and 7 depict the graph of the hybrid Multi-Hop RF/FSO system with the same structure $M=2$ and $N=3$ for various values of the parameter K and different turbulence intensity, respectively.

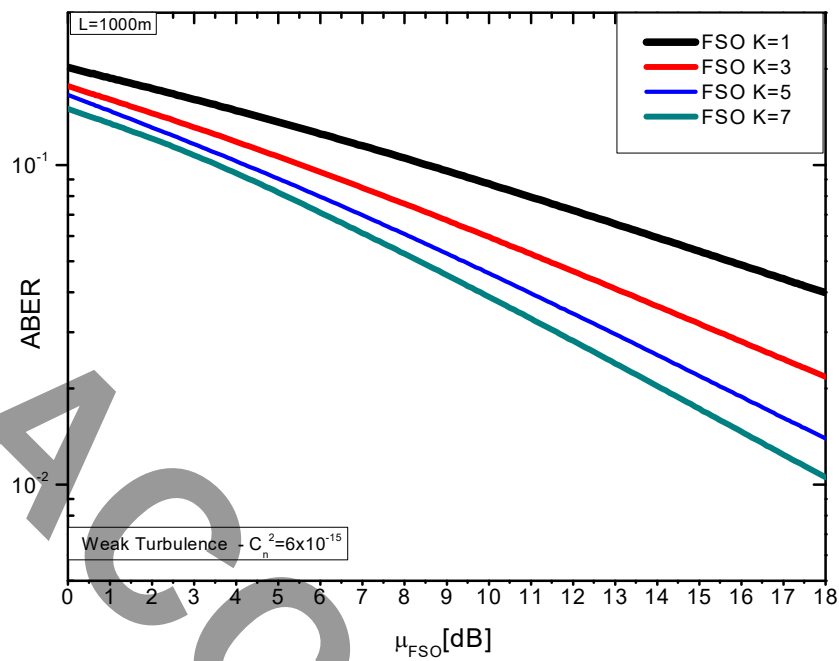


Figure 1. Determination of ABER as a function of the K factor for the FSO system.

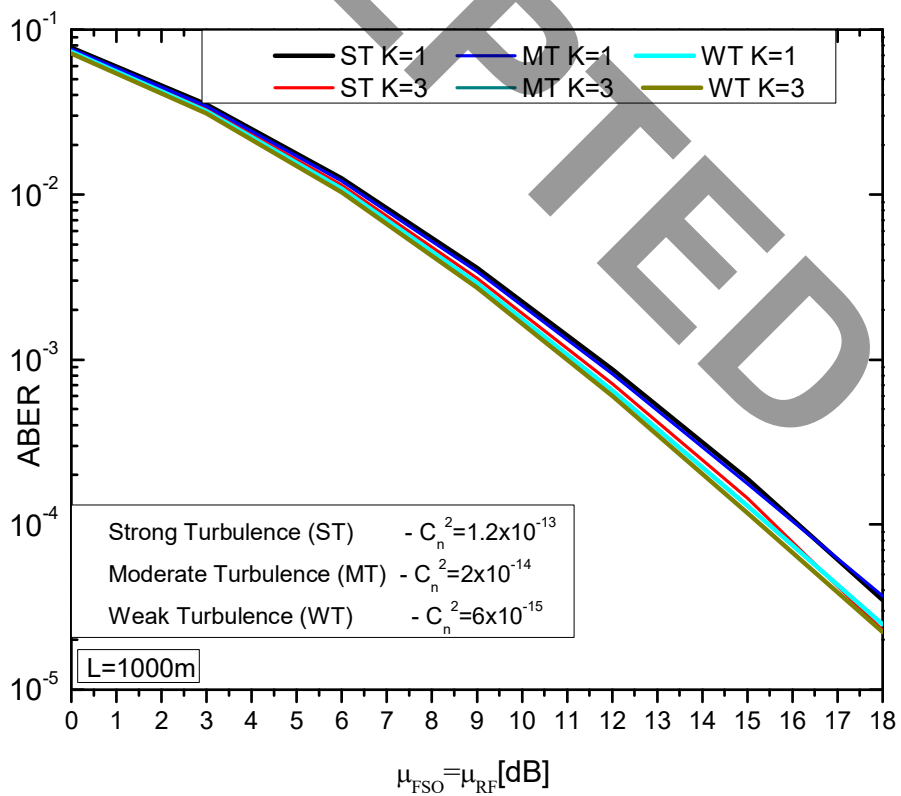


Figure 2. Determination of ABER as a function of the K factor for the One-Hop hybrid RF/FSO system.

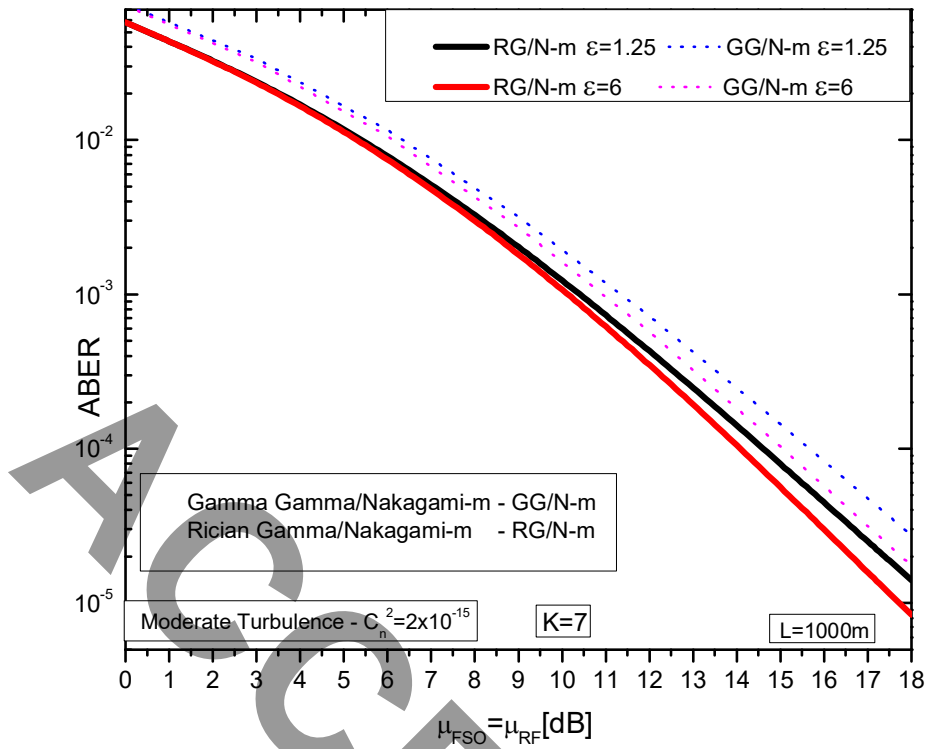


Figure 3. ABER relationship when using hybrid RF/FSO systems with Rician-Gamma distribution and Nakagami-m fading, and Gamma-Gamma distribution and Nakagami-m fading, depending on pointing error.

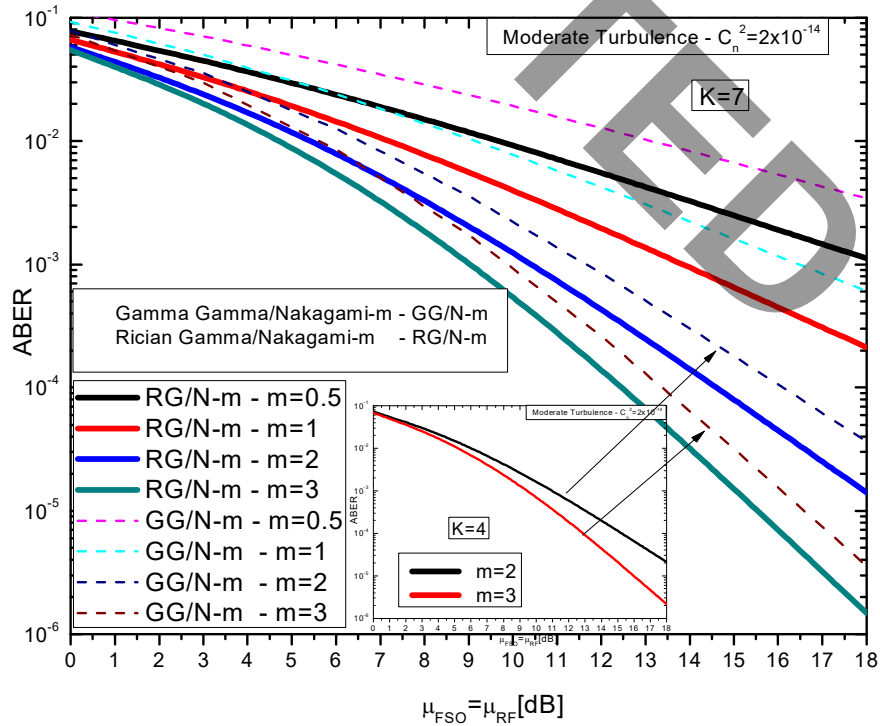


Figure 4. ABER analysis using Gamma-Gamma/Nakagami-m and Gamma-Rician/Nakagami-m models for hybrid One-Hop FSO/RF systems.

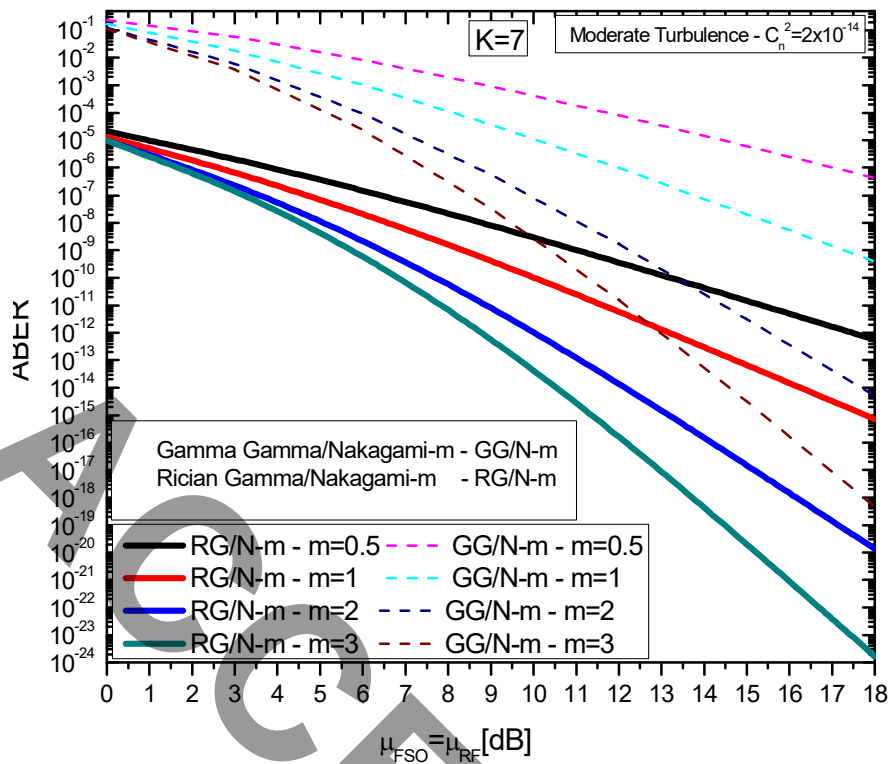


Figure 5. ABER analysis using Gamma-Gamma/Nakagami-m and Gamma-Rician/Nakagami-m models for hybrid Multi-Hop systems.

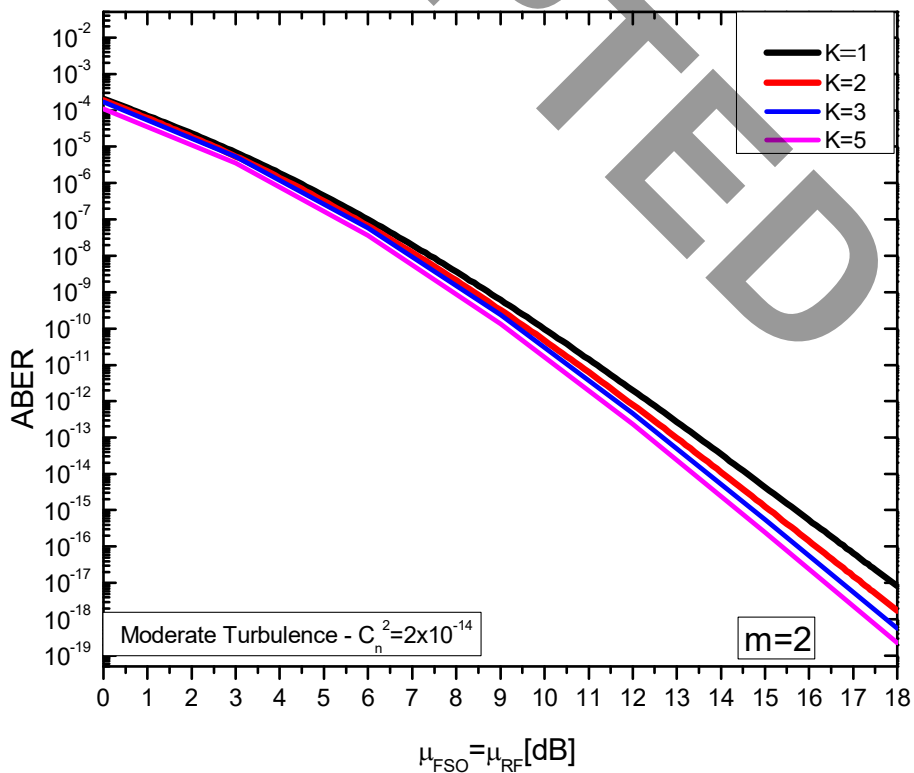


Figure 6. ABER analysis of the hybrid RF/FSO Multi-Hop system using the Gamma-Rician/Nakagami-m model, with a structure of 2 hops and 3 paths, as a function of K parameter.

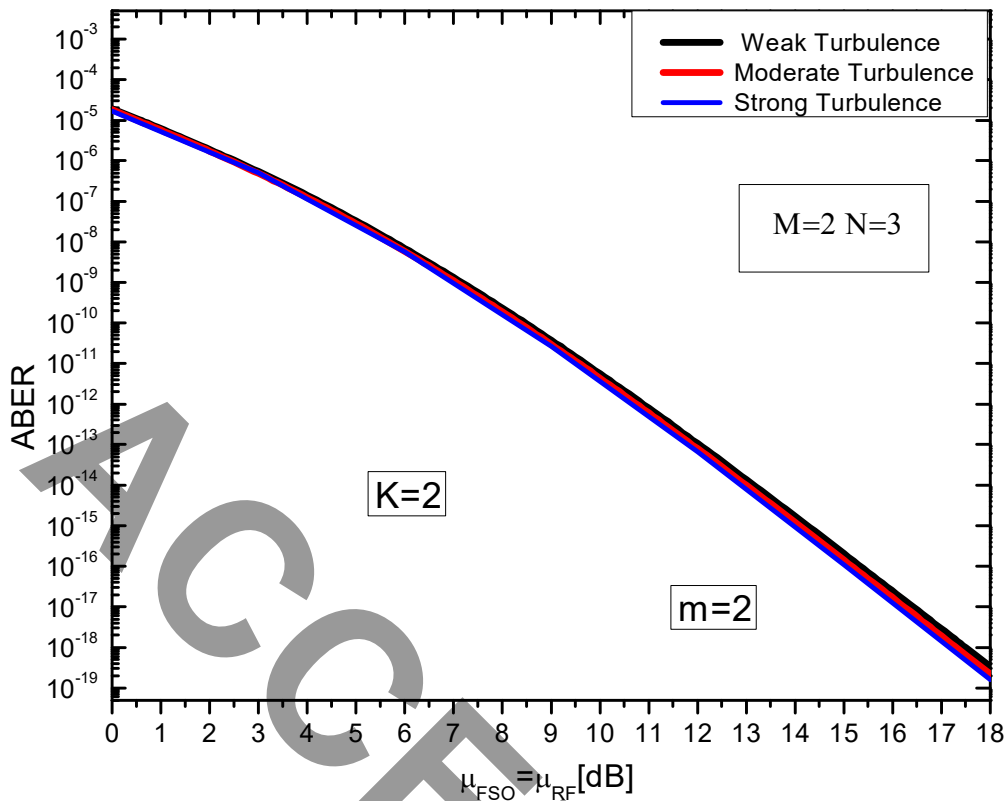


Figure 7. ABER analysis of the hybrid RF/FSO Multi-Hop system using the Gamma-Rician/Nakagami- m model, with a structure of 2 hops and 3 paths, as a function of the intensity of turbulence.

Similarly to One-Hop RF/FSO systems, in hybrid Multi-Hop RF/FSO systems, increasing the K parameter reduces the ABER value, thereby improving system performance. The K factor in this structure can also be a suitable parameter for fine-tuning the system when analyzing the impact of environmental conditions on RF/FSO system performance (Figure 6).

As expected, atmospheric turbulence does not have a significant impact on these systems. The results are even significantly better compared to One-Hop systems. The reason for these results is the resilience of the RF system under conditions of strong turbulence. When the performance of the FSO system deteriorates due to the presence of atmospheric turbulence, the RF system takes over the transmission, showcasing its evident resistance to atmospheric disturbances.

Figures 8 and 9 depict a graphical representation of ABER in hybrid Multi-Hop RF/FSO systems, depending on the relay structure of the system.

The analysis was performed under moderate turbulence, with parameters set at $K=2$ and $m=2$. As depicted in figure 8, maintaining a constant number of hops while increasing the number of paths results in a lower ABER, thereby enhancing system performance. This improvement is due to the selection of the signal with the highest SNR as the output, increasing the likelihood of choosing the maximum SNR when more paths are available. Thus, a signal with a higher SNR is more likely to be delivered to the receiver. Conversely, a configuration with a constant number of paths but an increased number of hops (figure 9) leads to a rise in ABER with each hop, adversely affecting system performance. Assuming stable conditions throughout the propagation distance, the ABER remains uniform after each hop. However, as the number of hops grows, so does the propagation distance, culminating in an increased cumulative ABER and, consequently, degrading the overall system performance.

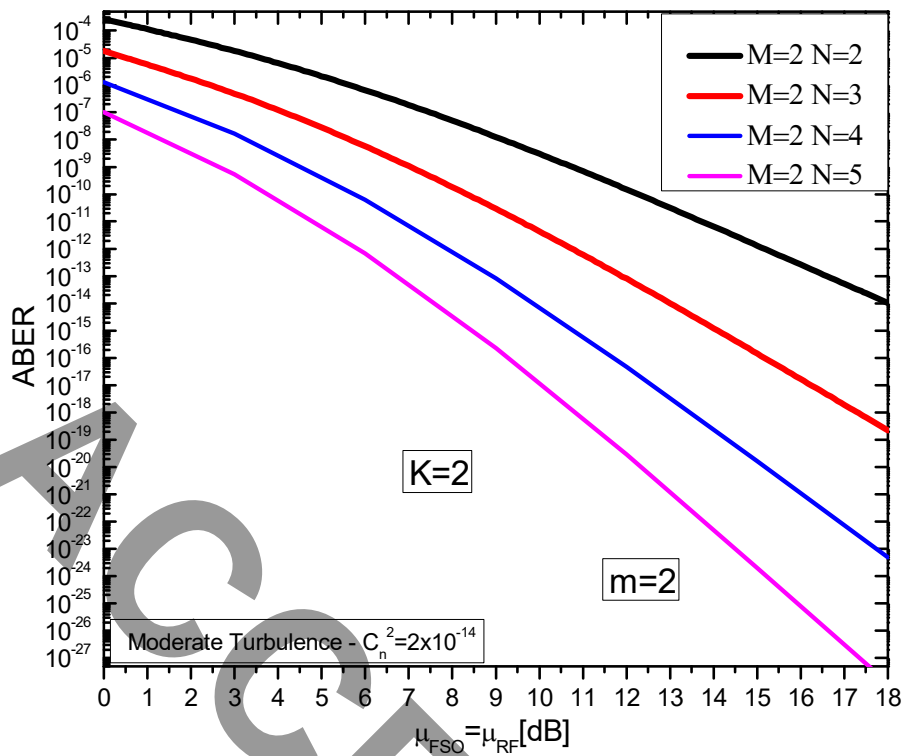


Figure 8. ABER analysis of hybrid RF/FSO Multi-Hop system using Gamma-Rician/Nakagami- m model with variable path structure and fixed hop structure.

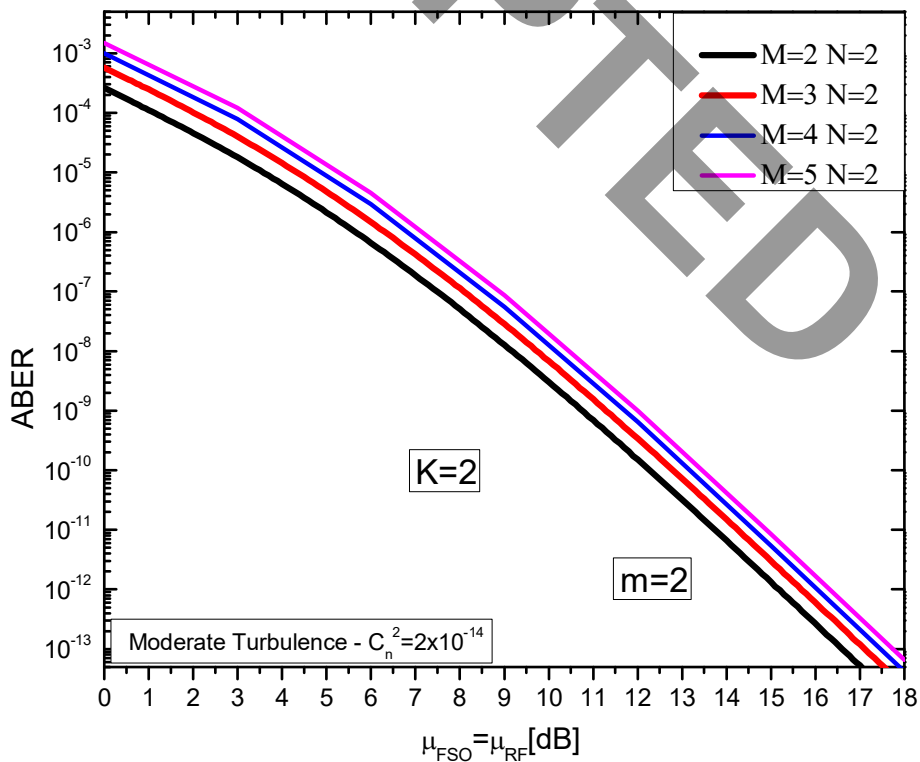


Figure 9. ABER analysis of hybrid RF/FSO Multi-Hop system using Gamma-Rician/Nakagami- m model with variable hop structure and fixed path structure.

5 Conclusion

In this paper, a comprehensive analytical model is presented for evaluating the performance of hybrid RF/FSO systems that integrate two independent statistical models. The Gamma-Rician model is utilised for modelling FSO turbulence, while the Nakagami- m distribution is applied to RF fading. An ABER analysis is conducted using the CBPSK modulation scheme, highlighting the advantages of the hybrid RF/FSO system. It was observed that the hybrid RF/FSO system, particularly in the One-Hop configuration, exhibits greater resistance to atmospheric turbulence and generally outperforms standalone FSO systems under similar weather conditions. Furthermore, the system was compared with the commonly used Gamma-Gamma/Nakagami- m model. ABER analysis of a parallel Multi-Hop hybrid RF/FSO system demonstrated resilience to atmospheric turbulence and the ability to fine-tune performance using the K factor and the m parameter of the fading distribution. Comparative analysis revealed that our model achieves superior results, especially in scenarios with lower electrical SNR. Overall, the hybrid RF/FSO system shows excellent performance, which can be further optimised by adjusting the K and m parameters along with the electrical SNR. Compared to the Gamma-Gamma/Nakagami- m model, our model offers superior characteristics, making it well-suited for precise system tuning to achieve desired performance levels across varying atmospheric conditions. This work significantly advances the understanding and analysis of hybrid RF/FSO systems and expands the range of statistical models available to streamline the implementation of RF/FSO systems.

References

- [1] M. Z. Chowdhury, M. K. Hasan, M. Shahjalal, M. T. Hossan, and Y. M. Jang, "Optical Wireless Hybrid Networks: Trends, Opportunities, Challenges, and Research Directions," *IEEE Communications Surveys & Tutorials*, vol. 22, no.2 pp. 930-966, 2020, doi: 10.1109/COMST.2020.2966855.
- [2] M. A. Khalighi, and M. Uysal, "Survey of Free Space Optical Communication Systems: Fundamental Principles and Applications," *IEEE Communications Surveys & Tutorials*, vol. 16, no. 4, pp. 2231-2258, 2014, doi:10.1109/comst.2014.2329501.
- [3] H. Elgala, R. Mesleh, and H. Haas, "Indoor Optical Wireless Communication: Potential and State-of-the-Art," *IEEE Communications Magazine*, vol.49, no.9, pp. 56-62, 2011, doi:10.1109/mcom.2011.6011734.
- [4] A. Sevincer, A. Bhattarai, M. Bilgi, M. Yuksel, and N. Pala, "Lightnets: Smart Lighting and Mobile Optical Wireless Networks – A Survey," *IEEE Communications Surveys & Tutorials*, vol.15, no. 4, pp. 1620-1641, 2013, doi:10.1109/surv.2013.032713.00150.
- [5] Z. Xu, and B. M. Sadler, (2008) "Ultraviolet Communications: Potential and State-of-the-Art," *IEEE Communications Magazine*, vol. 46, no. 5, pp. 67-73, 2008, doi:10.1109/mcom.2008.4511651.
- [6] A. Upadhyaya, M. Meenalakshmi, S. Chaturvedi, and V. K. Dwivedi, "Full duplex mixed FSO/RF relaying systems with self-interference and outdated CSI," *Optical and Quantum Electronics*, vol. 55, no. 3, 2023, doi:10.1007/s11082-022-04265-8.
- [7] S. Ghatwal, and H. Saini, "Correction to, Investigations on challenges faced by hybrid FSO/RF high-speed networks," *Journal of Optics*, vol. 52, pp. 935-936, 2022, doi:10.1007/s12596-022-00898-w.
- [8] W. M. R. Shakir, (2019) "On performance analysis of hybrid FSO/RF systems," *IET Communications*, vol. 13, no. 11, pp. 1677-1684. doi:10.1049/iet-com.2018.5147.
- [9] T. Rakia, H. C. Yang, M. S. Alouini, and F. Gebali, "Outage Analysis of Practical FSO/RF Hybrid System with Adaptive Combining," *IEEE Commun. Letters*, vol. 19, no. 8, pp. 1366-1369, 2015, doi:10.1109/lcomm.2015.2443771.
- [10] M. J. Saber, Z. Rezki, and M. S. Alouini, "Secrecy Performance Analysis of Mixed α - μ and Exponentiated Weibull RF-FSO Coop. Relaying System," *IEEE Access*, vol. 9, pp. 72342-72356, 2019, doi:10.1109/access.2021.3078610.
- [11] B. Helal, H. C. Yang, M. S. Alouini, and F. Gebali, "Practical Considerations and Performance Analysis of RF/FSO Hybrid Systems," *IEEE Access*, vol. 7, pp. 131418-131434, 2019, doi:10.1109/access.2019.2940630
- [12] Y. Wu, J. Chen, J. Guo, G. Li, and D. Kong, "Performance Analysis of a Multi-Hop Parallel Hybrid FSO/RF System over a Gamma-Gamma Turbulence Channel with Pointing Errors and a Nakagami- m Fading Channel," *In Photonics MDPI*, vol. 9, no. 9, pp. 631, 2022, doi:10.3390/photonics9090631

- [13] B. Bag, A. Das, I. S. Ansari, A. Prokeš, C. Bose, and A. Chandra, "Performance analysis of hybrid FSO systems using FSO/RF-FSO link adaptation," *IEEE Photonics Journal*, vol. 10, no. 3, pp. 1-17, 2018, doi:10.1109/jphot.2018.2837356
- [14] W. A. Alathwary, and E. S. Altubaishi, "On the performance analysis of decode-and-forward multi-hop hybrid FSO/RF systems with hard-switching configuration," *IEEE Photonics Journal*, vol. 11, no. 6, pp. 1-12, 2019, doi:10.1109/jphot.2019.2949859.
- [15] M. A. Amirabadi, and V. T. Vakili, "Performance comparison of two novel relay-assisted hybrid FSO/RF communication systems," *IET Communications*, vol. 13, no. 11, pp. 1551-1556, 2019, doi:10.1049/iet-com.2018.5469
- [16] <https://mathworld.wolfram.com>
- [17] J. Todorović, P. Spalević, S. Panić, B. Milosavljević, and M. Gligorijević, "FSO system performance analysis based on novel Gamma-Chi-square irradiance PDF model," *Optica Applicata*, vol. 51, no. 3, pp. 335-348, 2021, doi:10.37190/oa210303.
- [18] P. Wang, R. Wang, L. Guo, T. Cao, and Y. Yang, "On the performances of relay-aided FSO system over M distribution with pointing errors in presence of various weather conditions," *Optics Communications*, vol. 367, pp. 59-67, 2016, doi:10.1016/j.optcom.2016.01.004.
- [19] K. O. Odeyemi, and P. A. Owolawi, "Selection combining hybrid FSO/RF systems over generalized induced-fading channels," *Optics Communications*, vol. 433, pp. 159-167, 2019, doi:10.1016/j.optcom.2018.10.009
- [20] I. S. Ansari, S. Al-Ahmadi, F. Yilmaz, M. S. Alouini, and H. Yanikomeroğlu, "A new formula for the BER of binary modulations with dual-branch selection over generalized-K composite fading channels," *IEEE Transactions on Communications*, vol. 59, no. 10, pp. 2654-2658, 2011, doi:10.1109/tcomm.2011.063011.100303a.
- [21] E. Zedini, and M. S. Alouini, "Multihop relaying over IM/DD FSO systems with pointing errors," *Journal of Lightwave Technology*, vol. 33, no. 23, pp. 5007-5015, 2015, doi:10.1109/jlt.2015.2492244
- [22] M. A. Amirabadi, and V. T. Vakili, "Performance comparison of two novel relay-assisted hybrid FSO/RF communication systems," *IET Communications*, vol. 13, no. 11, pp. 1551-1556, 2019, doi:10.1049/iet-com.2018.5469.
- [23] W. H. Press, S. A. Teukolsky, W. A. Vetterling, and B. P. Flannery, (1992) "Numerical Recipes in C: The Art of Scientific Computing," *Cambridge University Press*, 1992, doi:10.1017/s0033583500004285